مجلة كلية التربية الاساسية
كلية التربية الاساسية – الجامعة المستنصرية
Journal of the College of Basic Education Vol.31 (NO. 131) 2025, pp. 1116-1133

A Mini-Review On The Fabrication Of Expanded Graphite And Its Metal Oxide Composites For The Photodegradation Of Dyes

[(1)] Sundus Hadi Merza
Department of Chemistry, College of Education for Pure Science / Ibn-Al-Haitham, University of Baghdad, Iraq
[1]sundus.h.m@ihcoedu.uobaghdad.edu.iq

Abstract:
This mini review provides an overview of methods for manufacturing expanded graphite (EGT) and the use of its composites with metal oxides in the field of photodegradation of dyes. Dyes from textile manufacturing represent a significant environmental pollution problem in waterways worldwide, highlighting the need for environmentally friendly and efficient technologies to remove dyes from industrial and local wastewater. Photodegradation technologies offer a low-cost, sustainable solution with minimal secondary pollution. Carbon-based materials, such as expanded graphite, are advantageous in enhancing catalytic activity. Accordingly, this review will explore the different fabrication techniques of expanded graphite and summarize the recent development of EGT-metal oxide composite in photocatalysis process towards environmental remediation application. From this study concludes that the photodegradation method using metal oxide-expanded graphite composite is an effective and cost-efficient option for degrading dyes.

Keywords: exfoliation; interlayer spacing; photocatalysis; pollutant; X-ray diffraction.

Introduction:

The dyeing industry, along with industrial and agricultural waste, contributes significantly to environmental pollution. The wastewater created from dyeing processes often contains hazardous chemicals that can cause severe health issues, affecting both aquatic and human life. Dyes, which are commonly toxic, carcinogenic, or mutagenic, pose serious threats to water quality, leading to reduced metabolic rates in aquatic organisms and various disturbance in humans, such as skin ulcers, nausea, and even bleeding (1–4) As such, effective and sustainable solutions for dye degradation are urgently required to safeguard human health and the environment. Numerous water purification techniques, including physical, biological, and chemical methods, have been developed to deal with dye contamination. While

physical methods like adsorption and ion exchange are commonly employed, they often require costly adsorbents, such as activated carbon, which are not always economically feasible [5] . Biological methods, which utilize bacteria and fungi, and chemical methods, such as chemical oxidation and solvent extraction, are typically slow and expensive [6]. Therefore, emerging technologies, particularly those involving nanomaterials, offer promising solutions for dye degradation due to their unique properties, including high surface area, reactivity, and efficiency.

Among these promising technologies is photocatalysis, a process where semiconducting materials specifically transition metal oxides (TMOs) like titanium dioxide (TiO_2), zinc oxide (ZnO), and manganese oxide (MnO_2), absorb photons to catalyze redox reactions. This process breaks down complex organic molecules, such as dyes, into simpler, non-toxic fragments [7]. Metal oxides are particularly valued for their catalytic activity, electrochemical properties, and stability, making them ideal candidates for photodegradation applications.

Expanded graphite (EGT) is a form of the layered natural graphite, its carbon atoms bonded covalently with a wealth of π-electrons [8]. EGT or graphite intercalation compounds (GICs) is a low density an inorganic porous carbon [9] can be designed by inserting types of chemical compound or called intercalants between the graphite layers. Intercalants can either be alkali metals, which act as electron donors, or iodine, which functions as an electron acceptor [10]. Van der Waals force is the binding force between graphite layers. EGT is created by destroyed van der Waals interaction by thermal or chemical treatments to exhibits a honeycomb microstructure with wrinkled graphene sheets, resulting in a high surface area, excellent flexibility, and superior thermal and electrical conductivity[11]. EGT has garnered significant attention due to its unique structure and remarkable properties. The use of oxidizing agents, such as potassium permanganate, nitric acid, and sulfuric acid, enhances the intercalation of functional groups between graphite layers, leading to an expanded form that is more reactive and easier to process [12] . The combination of expanded graphite with metal oxides results in composites that take advantage of the synergistic properties of both materials. These composites enhance the photocatalytic performance of metal oxides in dye degradation. As a result, EGT-metal oxide (MO) composites are gaining increasing attention in environmental remediation, including in the photodegradation of dyes. This mini-review aims to explore the fabrication methods of expanded graphite (EGT), with a particular focus

on the role of its metal oxide composites in the efficient photodegradation of dyes, contributing to sustainable water treatment solutions.

Synthesis method and structural characterization of EGT.

Researchers have explored different methods for synthesizing EGT included, chemical and physical methods such as chemical intercalation, oxidation and electrochemical method, thermal expansion under low or high temperature expansion, microwave expansion and ultrasonic methods [13]. The following section reviews their approaches, highlighting the methods that employed and the key findings of their studies.

Ting et al [14] prepared expanded graphite at room temperature (RTEG). The method was carried out by adding natural graphite (NG) to ultrasonication system consist of ammonium persulfate $(NH_4)_2S_2O_8$ and concentrated sulfuric acid. RTEG showed an expansion volume up to 225 times with a worm-like structure [Figure 1].

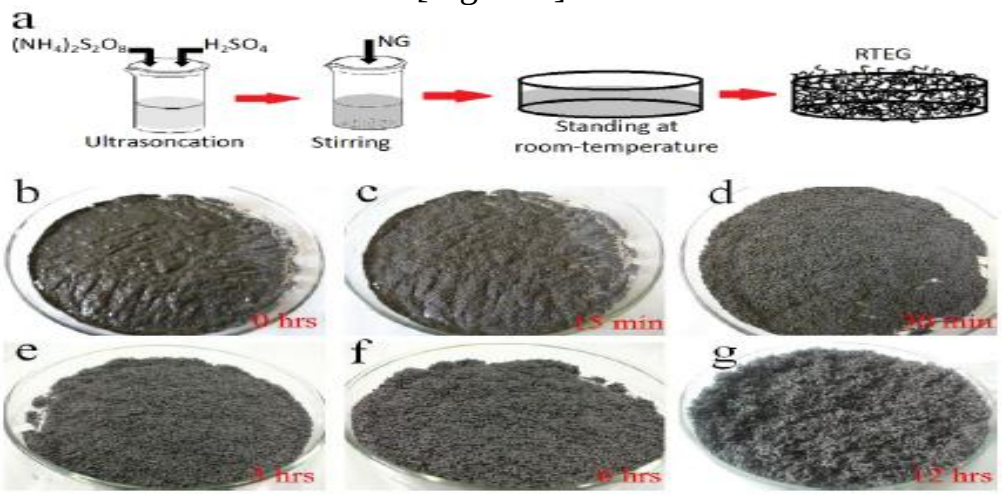

Figure 1: (a) A schematic of the RTEG preparation process and (b-g) optical images showing the morphological evolution of NG over time.

Additionally, the (002) diffraction peak of the RTEG shifted to the left and became weaker than NG disorder suggestion increase the interlayer spacing and exfoliation of the graphite layers. The morphological features of the samples were investigated using Field-emission scanning electron microscopic (FESEM) [Figure 2]. The form of the natural graphite changed from a closely stacked layered configuration to fully expansion or worm-like.

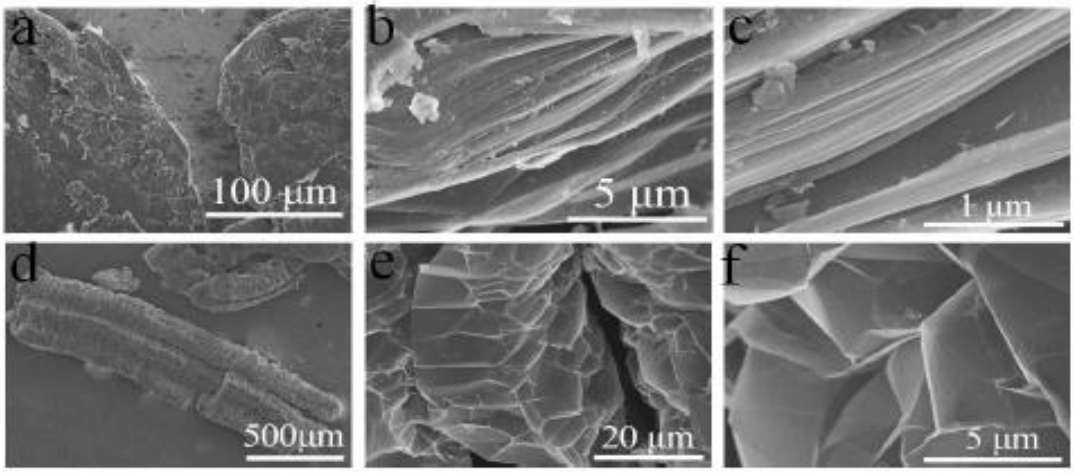

Figure 2: FESEM images of (a-c) NG and (d-f) RTEG.

Avinash et al. [15] prepared expanded graphite (EG) using natural graphite flakes. A binary blend of concentrated sulfuric acid (70 ml) and concentrated nitric acid (30 ml) was used to prepare graphite intercalation compound (GIC). A rapid expansion at 800 c° in a muffle furnace was used to form EG [Figure 3].

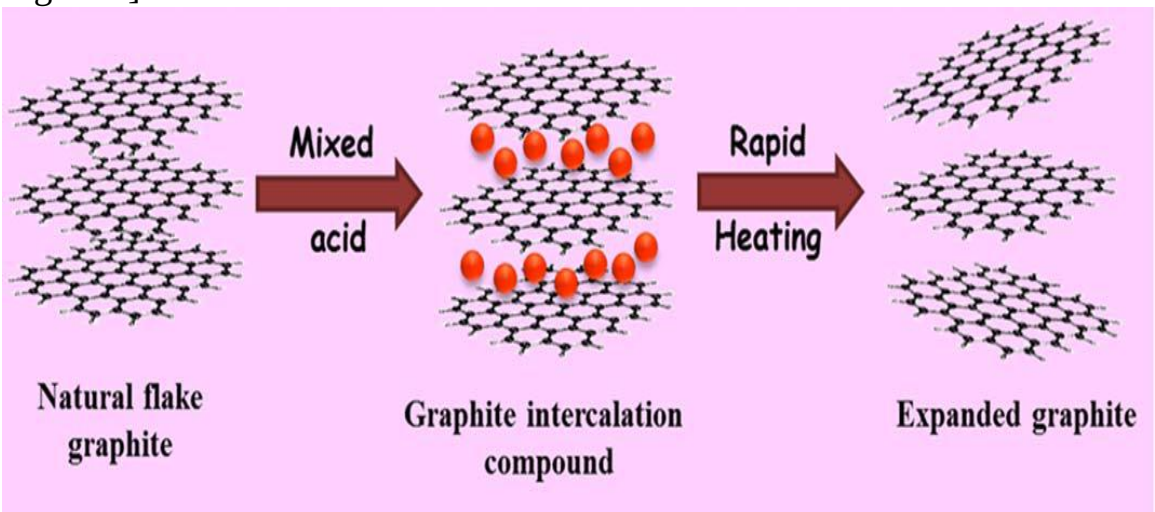

Figure 3: Preparation of EGT from natural flake graphite.

Asghar et al. [16] synthesized graphite intercalation compounds (GIC) with low sulfur content, specifically bisulfate-intercalated graphite, using Chinese natural flake graphite (CNFG) as precursor in the electrochemical system [Figure 4 f]. The anode composed of graphite paste 50% w/w (graphite with a diluted H_2SO_4 solution) and cathode from 316 stainless steels. An acid treated of aqueous solution of NaCl (brine 0.3% w/w) was utilized in the cathode partition. The electrochemically prepared (1g, GIC) was exposed to

temperature shock between 800°C and 900°C for 1 minutes to assess changes in bulk volume. The prepared GIC was confirmed through X-ray diffraction (XRD). Diffraction of the crude graphite was observed at 2θ = 26.6°, with an equivalent d-spacing of 3.35 Å. The peaks observed for electrochemically treated CNFG and thermally exfoliated graphite appeared at 2θ = 24° (d = 3.7 Å) and 2θ = 27.2°, suggesting the construction of a novel crystal structure. The scanning electron microscope (SEM) was utilized to examine the morphologies of CNFG, prepared GIC, and delaminated graphite. CNFG exhibited a characteristic crystalline graphite structure with platelets featuring smooth, flat surfaces. In contrast, exfoliated GICs with varying ordinary particle sizes (A = 100 µm, B = 184 µm, C = 347 µm, and D = 484 µm) displayed linear expansion within the graphite crystal structure [Figure 4].

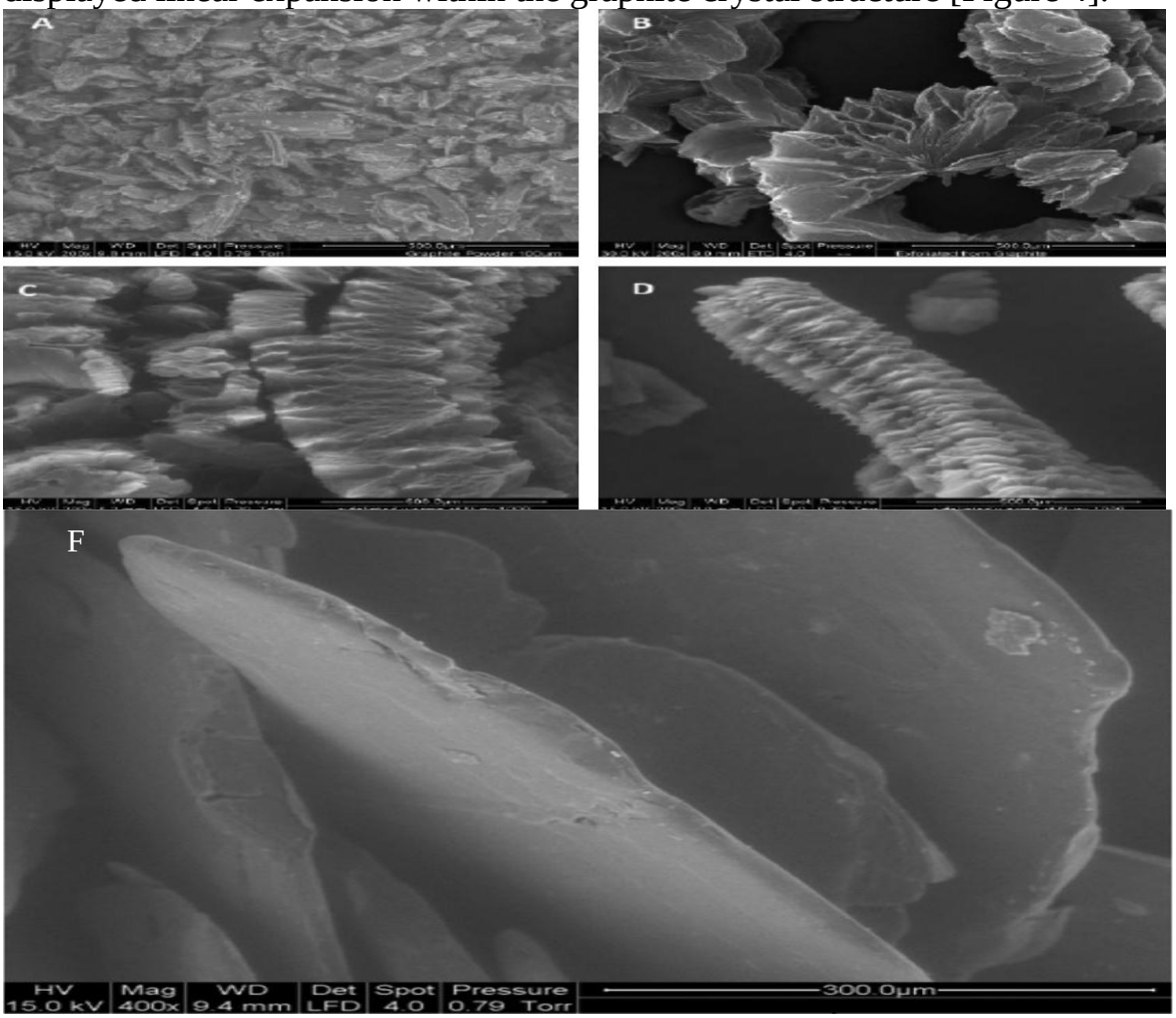

Figure 4: SEM images of exfoliated GICs as a function of ordinary particle size (A = 100 mm; B = 184 mm; C = 347 mm and D = 484 mm) and (F) SEM image of CNFG at 400 magnifications.

Guojun et al. [17] synthesized EGT by blending natural flake graphite (NFG) with different ratio of intercalators $K_2Cr_2O_7$, CH_3COOH, HNO_3 and $HClO_4$ at room temperature. Consequently, intercalated graphite was exposed to temperatures ranging from 300 to 900 °C for 5 (s) at muffle furnace. SEM images of NFG
revealed that the layers are tightly arranged in a lamellar structure. High-temperature expansion of graphite significantly alters its structure. At temperatures between 300–350°C, intercalated reagents cause the graphite layers to strip along the c-axis, increasing layer spacing with minimal deformation. At 450°C, the sheets begin to bend, creating a "bulging" effect. As the temperature rises further, the graphite structure transforms from lamellar stripping to a more curled sheet configuration.

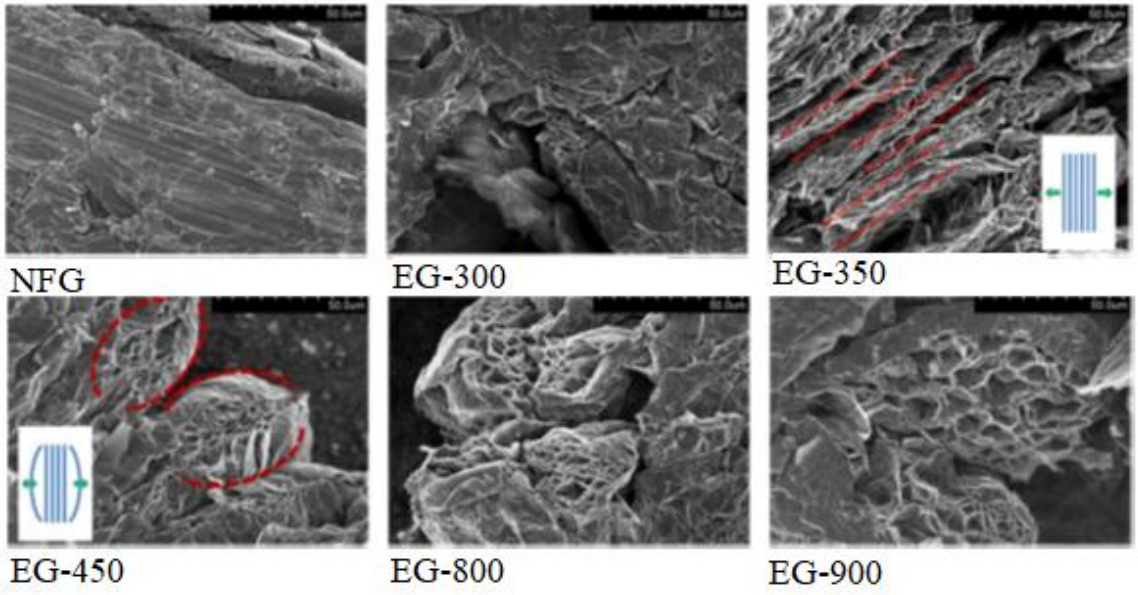

Figure 5: The morphology of NFG and EGs in SEM analysis

Han-Yu Li et al. [18] prepared expanded graphite foil (EGF) by using electrochemical expansion process of graphite foil (GF). A piece of GF and a Pt strip served as the working and counter electrodes, respectively, dipped in 0.1 M of $(NH_4)_2SO_4$ electrolyte solution. The two parallel electrodes were placed at a distance of 2 cm from each other. To induce electrochemical expansion, a DC voltage of +10 V was applied to the GF electrode for 0, 1, 3, 5, 7, and 10 minutes. FESEM was used to studied the microstructure and morphology. The high-magnitude SEM image revealed that the worm-like strips were composed of several layers of disordered graphene sheets, with numerous bubbles, approximately 40 nm in diameter.

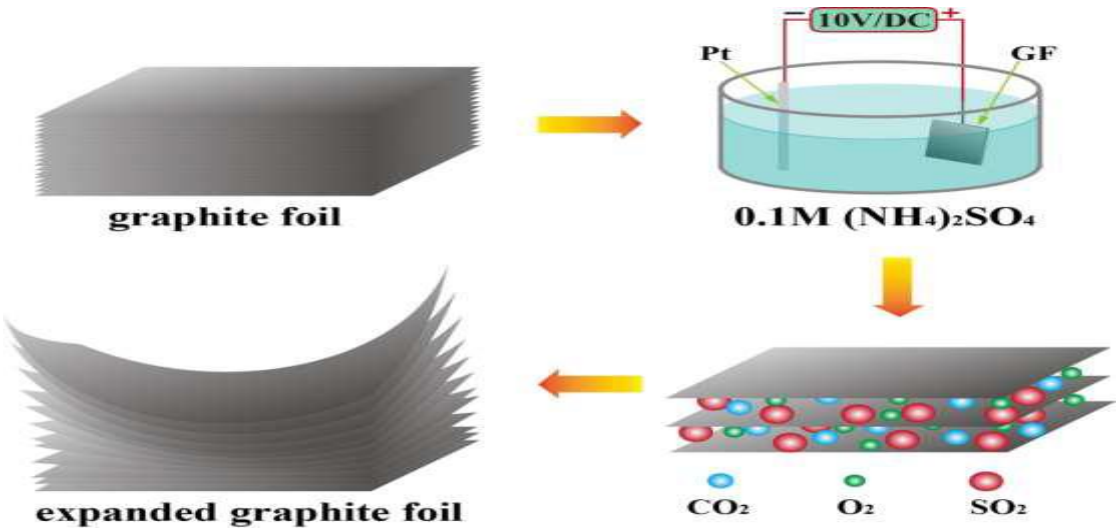

Figure 6: The fabrication of flexible EGF electrode.

Ying-Liang Chen et al. [19] Firstly, prepared a GIC by chemical intercalation process using mixture of $(NH_4)_2S_2O_8$ as an oxidizing agent and concentrated H_2SO_4 as an intercalating agent. An oxidizing agent and an intercalating material were mixed by using an ultrasonic bath. Secondly, EGTs was prepared by expansion the intercalates into gases by varied power microwave radiation and time. SEM image of the surface of graphite appeared a flaky and a smooth with size in range of 300– 600 μm. Also found that the surface of GIC became rougher than the GT and have a layered structure. Moreover, all EGTs samples that were prepared by exposure GIC to microwave power, 200 W, 500 W, and 800 W for 60 s showed worm or vermicular -like structures.

Son et al. [20] investigated the thermal exfoliation of expandable graphite (EG0) from 0 to 800 ºC, preparing seven different expanded graphite (EG) samples to regulate the high volume of expansion and interlayer spacing. According to SEM analysis, the SEM image of EG0 revealed lamellar structures with well-defined shapes, alongside graphene sheet structures that lacked open or semi-open inner pores. At 600 ºC, graphite underwent volume exfoliation, expanding by 80 to 100 times and resulting in the creation of a distinct worm- shaped structure. This study provides emerging insights into creation and advancement of EG, with a reduction in d-spacing observed at the most favorable thermal exfoliation temperature of 600 ºC. The XRD patterns of expanded graphite at different expansion times (EG1–EG60) showed distinct diffraction peaks at $2\theta = 26.3°$, while the diffraction peak of EG0 at $2\theta = 26.03°$ appeared broad. This peak corresponds to the (002) plane, resulting in an interlayer spacing (d-spacing) of 3.422 Å (~0.3422 nm),

which aligns well with the typical diffraction pattern for graphite. Furthermore, the EG1–EG60 samples exhibited a smaller diffraction peak at a lower 2θ value of 54.6°, attributed to the (004) plane, compared to EG0 (2θ = 54.84°), suggesting enhanced crystallinity in the calcined EG samples. With an increase in exfoliation time from 1 to 60 minutes, the (002) plane diffraction peak for most EG samples shifted from 2θ = 26.03° to 26.34°, while the EG30 and EG60 samples exhibited a shift to 2θ = 26.4°.

Tiefeng Peng et al. [21] prepared sulfur-free expandable graphite (EGT) from natural flake graphite (NFG) using oxidative intercalation with potassium permanganate ($KMnO_4$), perchloric acid ($HClO_4$), and ammonium nitrate (NH_4NO_3). These reagents facilitated oxidation, inducing significant structural changes in the graphite. The EGT sample was exposure to high temperature at 400 °C for 5 minutes. X-ray diffraction (XRD) analysis revealed a decrease in peak intensity and increased peak broadening, indicating a loss of crystallinity and structural modifications. The splitting of the d_{002} and d_{004} peaks and the shift of the diffraction peak to a lower 2θ value confirmed the oxidation-induced expansion of graphite. Initially, NFG exhibited a compact, lamellar structure, but after oxidation, the graphite layers became more spaced out, thinner (several hundred nanometers), and curled at the edges. The transformation led to a worm-like structure, and the volume increased due to the formation of a porous internal structure with interconnected slit and slit-wedge shaped pores. These changes highlight how oxidation and intercalation processes significantly alter the graphite's properties, resulting in a highly expanded and porous material suitable for applications like flame retardants and energy storage.

Goudarzi and Hashemi Motlagh [22] prepared various EGT samples from graphite intercalated compound (GIC) with particle sizes of 35, 50, 80, and 200 mesh by heating them in an electrical furnace at temperatures of 700, 800, and 900 °C. nitrogen adsorption and SEM have been considered to study the volume and pore size and volume. The FT-IR analysis indicated that the EGT structure lacks oxygen-containing functional groups such as carboxyl and epoxy groups. The mercury porosimetry analysis demonstrated a diverse range of total pore areas for the expandable graphites (EGTs), spanning from 5 to 31 m^2/g. It was noted that both the particle size of the graphite intercalation compound (GIC) and the exfoliation temperature had a significant impact on the pore size distribution of the EGT. It was observed that a decrease in exfoliation temperature led to a reduction in sorption capacity. Additionally, expandable graphite (EGT) samples derived from

graphite intercalation compounds (GICs) at smaller scales of particle size exhibited diminished sorption capacities. Also, the SEM image of EGT specimen prepared from small GIC size and exfoliated at 900 °C for 30 s showed decreasing in the number of the exfoliated layers or compacted in the accordions structure. Various methods were used to prepare EGT are given in Table 1.

EGT- MO hybrids in photodegradation of dyes.

The hybrids MO and EGT created outstanding hierarchical composites, which are regarded as a promising alternative for enhancing the photocatalytic performance under both UV and visible light irradiation. The enhancement of the photocatalytic performance of the hybrids is attributed to the combined advantages of each component. MO have distinctive characteristics such as a huge surface-to-volume ratio that increased its adsorption capacity and reactivity [27].

The following section will discuss the photocatalysis of EGT-based metal

Table 1: Methods and XRD structural characterization of EGT.

Materials	GT	EGT	Structure	method	Ref.
H_2SO_4+$K_2S_2O_8$	2θ= 26.50° d =0.3362	2θ = - d= 0.3338	worm-like fluffy shape	Chemical method at 80 °C	[23]
H_2O_2+ $KMnO_4$.	2θ =26.6° *d* = 0.332	2θ = 25.2° *d* = 0.351°	increase in the interlayer spacing	Chemical method	[24]
Mixture of H_2SO_4 80 wt. % with HNO_3 +$KMnO_4$	2θ =26.2°	2θ =26.2° with lower intensity than GT	worm or accordion-like	exfoliation at 900 °C	[25]
NG, $KMnO_4$, $HClO_4$ and $(CH_3CO)_2O$ at weight ratios of 1:0.5:1:0.4	2θ =28.6° and 54.68°	2θ = 26.6°	wrinkles, packed layers with furrows and inner porous structure	microwave irradiation (720 W and 40 s)	[26]

oxide nanoparticles. Photocatalysis is one of the many nanotechnologies employed to improve pollutant removal efficiency, alongside methods such

as adsorption [28], ozonation [29], membrane separation [30], ultrafiltration membranes [31], electrodialysis [32] , and electrocoagulation [33]. The photocatalytic degradation of organic pollutants in wastewater has gained significant attention due to its cost-effectiveness, non-toxicity, abundant resources, and high catalytic activity under solar energy. Photocatalysis reaction accelerates the definite redox (photoreduction-photooxidation) reactions with the illuminated semiconductors. Presence EGT, play as support structure for the immobilization of heterogeneous photocatalysts, inhibits the recombination of electron (e^-) and hole (e^+) pairs, and extends light absorption into the visible range, as illustrated in Figure 7.

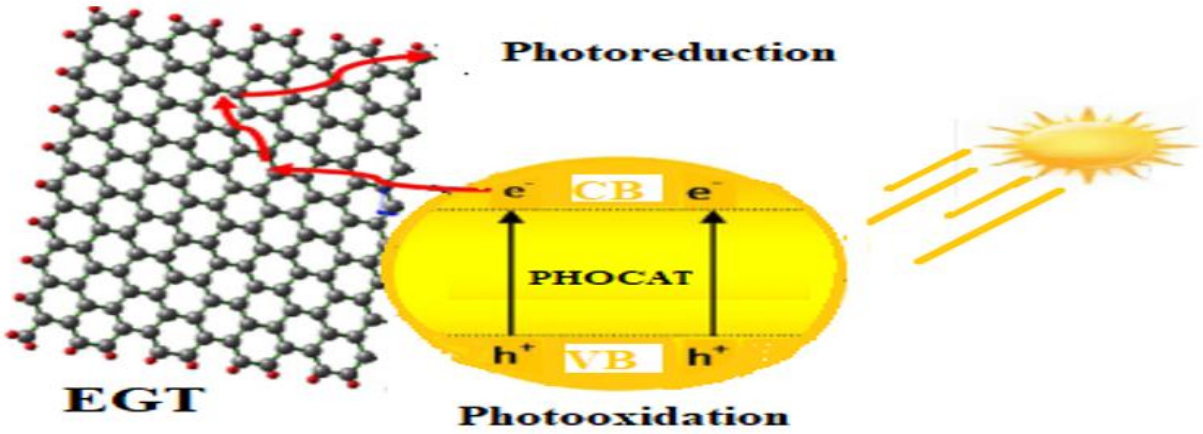

Figure 7: Role of EGT in photodegradation process

Three main stages are involved in the photocatalytic degradation mechanism: First, when the incident light reaches or exceeds the bandgap of the photocatalyst (PHOCAT) such as MO, charge carriers—electrons and holes—are generated. Upon excitation, electrons are promoted from the valence band (VB), resulting in the formation of holes in the valence band, while the excited electrons move to the conduction band (CB). Next, these charge carriers are adequately distributed across the photocatalytic surface. Lastly, redox reactions, including reduction and oxidation, occur on the surface of the photocatalyst. When organic pollutants engaged with photocatalyst materials, two reactions happened: first, the holes (h^+) react with H_2O or OH^- to formed $OH^\cdot$ free radical. Secondly, the excited electrons react with oxygen to form species of super oxygen radical $O_2^{\cdot-}$ as illustrated in Figure 8 and equations below [34].

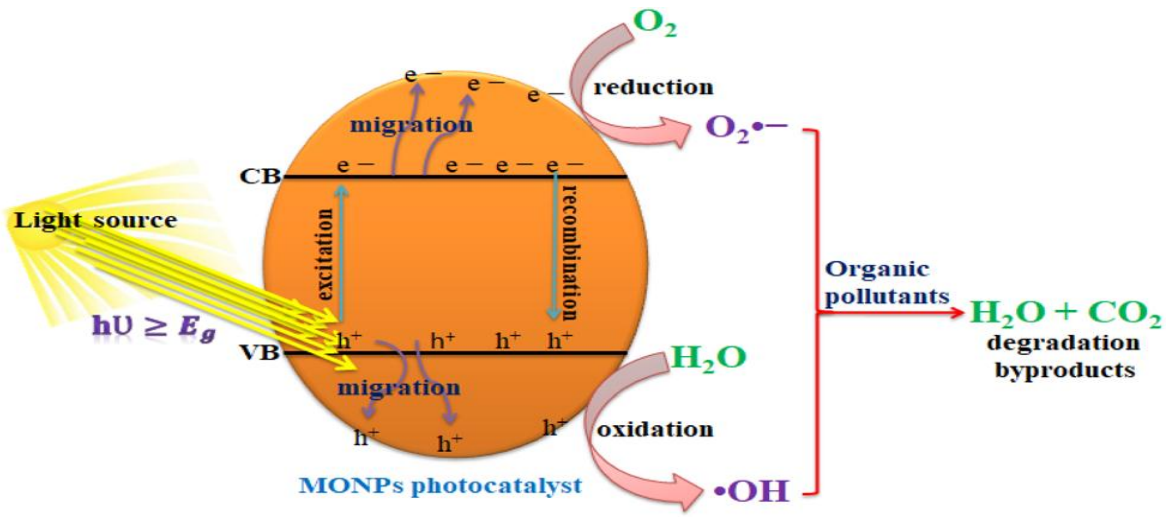

Figure 8: schematic photocatalysis mechanism [34] .

$$PHOCAT + h\upsilon \rightarrow PHOCAT\ (e^-)_{CB} + PHCAT\ (h^+)_{VB} \quad (1)$$

$$PHOCAT\ (h^+)_{VB} + H_2O \rightarrow H^+ + OH \quad (2)$$

$$PHOCAT\ (e^-)_{CB} + O_2 \rightarrow O_2^{-} \quad (3)$$

The extremely reactive free radicles formed in Eq.2 and Eq.3 degrade the organic pollutants that absorbed on the surface of the photocatalyst incomes to water and carbon dioxide. The reduction- oxidation reaction on the external surface of the PHCAT occurs due to the reaction of pollutant with holes to formed oxidation products and electrons to formed reduction products. Table 2 tabulated the photodegradation of organic pollutants by EGT-MO as photocatalyst.

Table 2. EGT-MO based photocatalysts for the photodegradation of pollutants.

Photocatalysts	Synthesis methods	Pollutants	Light	Reaction time	Degradation %	Ref
ZnO/EGT	Facial mixing	Methyl orange	Mercury lamp (30 W)	3h	94	[35]
ZnO/ EGT	Facial mixing	Malachite green	UV 8W (λ=254 nm) Visible	3h	99.04 94.06	[36]

			100W (λ=400)			
ZnO/ EGT	Oxidation of graphite with ZnSO4	Auramine lake yellow O	UV (20W) λ=200-275nm	Different time	15 at 50 $mg.L^{-1}$ 35 at 400 $mg.L^{-1}$	[37]
TiO_2/ EGT	sol-gel	Methylene blue	UV lamp (λ=356 nm), 1.2 mW/cm^2	Different time	96%	[38]
TiO_2/ EGT	sonication	Eosin yellow	Solar and Xenon lamp (500 W)	15 min	46.01	[39]
TiO_2/ EGT	sol-gel	Phenol	Xenon arc lamp (350 W)	Different time	46.6% at pH 3 96.3% at pH 7	[40]

Conclusion:

This mini review presented a details exploration about fabrication methods of expanded graphite (EGT) with metal oxide emphasized on their application in the photodegradation of dyes. EGT has a degree of separation between adjacent carbon layers. The separation of the layers results in cell wall consisting of multiple carbon layers, worm or accordion-like structure. sulfuric acid is the most widely intercalator species that used for preparing EGT. Photocatalysis approached for eliminating dyes from wastewater are reviewed in this article utilizing the composite of different metal oxide as photocatalytic nanomaterials.

A wide variety of metal oxides nanostructured and their composites have recently gained substantial curiosity as photocatalytic materials for degrading dyes or changing them into harmless products. Metal oxide and EGT composites have been verified to be operative photocatalysts for the interruption of organic pollutants when exposed to light.

Further Work

Further studies should be aimed towards evaluating the performance of EGT-metal oxide in the photodegradation multicomponent pollutant mixtures like

various dyes, pesticides, and pharmaceuticals in the real industrial wastewaters.

Acknowledgment

The authors are grateful for the support from Department of Chemistry / College of Pure Science (Ibn Al-Haitham) / University of Baghdad.

References

1. Wang Y, Sun X, Xian T, Liu G, Yang H. Photocatalytic purification of simulated dye wastewater in different pH environments by using BaTiO3/Bi2WO6 heterojunction photocatalysts. Optical Materials [Internet]. 2021;113(January):110853. Available from: https://doi.org/10.1016/j.optmat.2021.110853

2. Daneshvar N, Ashassi-Sorkhabi H, Tizpar A. Decolorization of orange II by electrocoagulation method. Separation and Purification Technology. 2003;31(2):153–62.

3. Donkadokula NY, Kola AK, Naz I, Saroj D. A review on advanced physico-chemical and biological textile dye wastewater treatment techniques. Reviews in Environmental Science and Biotechnology [Internet]. 2020;19(3):543–60. Available from: https://doi.org/10.1007/s11157-020-09543-z

4. Kishor R, Purchase D, Saratale GD, Saratale RG, Ferreira LFR, Bilal M, et al. Ecotoxicological and health concerns of persistent coloring pollutants of textile industry wastewater and treatment approaches for environmental safety. Journal of Environmental Chemical Engineering [Internet]. 2021;9(2):105012. Available from: https://doi.org/10.1016/j.jece.2020.105012

5. Choy KKH, McKay G, Porter JF. Sorption of acid dyes from effluents using activated carbon. Resources, Conservation and Recycling [Internet]. 1999 Jul;27(1–2):57–71. Available from: https://linkinghub.elsevier.com/retrieve/pii/S0921344998000858

6. CRINI G. Non-conventional low-cost adsorbents for dye removal: A review. Bioresource Technology [Internet]. 2006 Jun;97(9):1061–85. Available from: https://linkinghub.elsevier.com/retrieve/pii/S0960852405002452

7. Ullah R, Dutta J. Photocatalytic degradation of organic dyes with manganese-doped ZnO nanoparticles. Journal of Hazardous Materials [Internet]. 2008 Aug;156(1–3):194–200. Available from: https://linkinghub.elsevier.com/retrieve/pii/S030438940701761X

8. Wang LC, Ni X jiong, Cao YH, Cao G qun. Adsorption behavior of

bisphenol A on CTAB-modified graphite. Applied Surface Science [Internet]. 2018;428:165–70. Available from: http://dx.doi.org/10.1016/j.apsusc.2017.07.093
9. Tian Y, Zhang N, Liu Y, Chen W, Lv R, Ma H. Adsorption performance of expanded graphite and its binary composite microbeads toward oil and dyes. Desalination and Water Treatment. 2020;178:283–95.
10. Lambin P, Fink J. Electronic States of Carbon Materials. In: Reference Module in Materials Science and Materials Engineering [Internet]. Elsevier; 2016. p. 1–9. Available from: https://linkinghub.elsevier.com/retrieve/pii/B9780128035818010304
11. Chung DDL. A review of exfoliated graphite. Journal of Materials Science. 2015;51(1):554–68.
12. Salvatore M. Synthesis and Characterization of Expandable Graphite using different Oxidizing Agents. University of Naples Federico, Department of Chemical, Materials and Production Engineering. 2017;134.
13. Zhang D, Tan C, Zhang W, Pan W, Wang Q, Li L. Expanded Graphite-Based Materials for Supercapacitors: A Review. Molecules [Internet]. 2022 Jan 21;27(3):716. Available from: https://www.mdpi.com/1420-3049/27/3/716
14. Liu T, Zhang R, Zhang X, Liu K, Liu Y, Yan P. One-step room-temperature preparation of expanded graphite. Carbon [Internet]. 2017 Aug;119:544–7. Available from: https://linkinghub.elsevier.com/retrieve/pii/S0008622317304438
15. Barkoula NM, Alcock B, Cabrera NO, Peijs T. Flame-Retardancy Properties of Intumescent Ammonium Poly(Phosphate) and Mineral Filler Magnesium Hydroxide in Combination with Graphene. Polymers and Polymer Composites. 2008;16(2):101–13.
16. Asghar HMA, Hussain SN, Sattar H, Brown NW, Roberts EPL. Environmentally friendly preparation of exfoliated graphite. Journal of Industrial and Engineering Chemistry. 2014;20(4):1936–41.
17. Yin G, Sun Z, Gao Y, Xu S. Preparation of expanded graphite for malachite green dye removal from aqueous solution. Microchemical Journal [Internet]. 2021 Jul;166(March):106190. Available from: https://linkinghub.elsevier.com/retrieve/pii/S0026265X21002745
18. Li HY, Yu Y, Liu L, Liu L, Wu Y. One-step electrochemically expanded graphite foil for flexible all-solid supercapacitor with high rate performance. Electrochimica Acta [Internet]. 2017;228:553–61. Available from: http://dx.doi.org/10.1016/j.electacta.2017.01.063

19. Chen YL, Hsiao CH, Ya JY, Hsieh PY. Preparation of expanded graphite with (NH4)2S2O8 and H2SO4 by using microwave irradiation. Journal of the Taiwan Institute of Chemical Engineers [Internet]. 2024;154(1):105026. Available from: https://doi.org/10.1016/j.jtice.2023.105026
20. Son D-K, Kim J, Raj MR, Lee G. Elucidating the structural redox behaviors of nanostructured expanded graphite anodes toward fast-charging and high-performance lithium-ion batteries. Carbon [Internet]. 2021 Apr;175:187–201. Available from: https://linkinghub.elsevier.com/retrieve/pii/S0008622321000178
21. Peng T, Liu B, Gao X, Luo L, Sun H. Preparation, quantitative surface analysis, intercalation characteristics and industrial implications of low temperature expandable graphite. Applied Surface Science [Internet]. 2018;444:800–10. Available from: https://doi.org/10.1016/j.apsusc.2018.03.089
22. Goudarzi R, Hashemi Motlagh G. The effect of graphite intercalated compound particle size and exfoliation temperature on porosity and macromolecular diffusion in expanded graphite. Heliyon [Internet]. 2019;5(10):e02595. Available from: https://doi.org/10.1016/j.heliyon.2019.e02595
23. Hou B, Sun H, Peng T, Zhang X, Ren Y. Rapid preparation of expanded graphite at low temperature. New Carbon Materials [Internet]. 2020 Jun;35(3):262–8. Available from: https://linkinghub.elsevier.com/retrieve/pii/S1872580520604887
24. Lee HI, Kim WJ, Heo YJ, Son YR, Park SJ. Control of interlayer spacing of expanded graphite for improved hydrogen storage capacity. Carbon Letters. 2018;27(1):117–20.
25. Hossein S, Grigoryan G, Sarkeziyan V, Javad A. Characterization of Sol-Gel Derived CuO / SiO 2 Nanostructure on. International Journal of Industrial Chemistry. 2011;02(02):123–30.
26. Hoang NB, Nguyen TT, Nguyen TS, Bui TPQ, Bach LG. The application of expanded graphite fabricated by microwave method to eliminate organic dyes in aqueous solution. Cogent Engineering [Internet]. 2019;6(1). Available from: https://doi.org/10.1080/23311916.2019.1584939
27. Johar MA, Afzal RA, Alazba AA, Manzoor U. Photocatalysis and Bandgap Engineering Using ZnO Nanocomposites. Advances in Materials Science and Engineering. 2015;2015:1–22.
28. Collazzo GC, Jahn SL, Foletto EL. Removal of direct black 38 dye by adsorption and photocatalytic degradation on TiO2 prepared at low

temperature. Latin American Applied Research. 2012;42(1):55–60.
29. Quan X, Luo D, Wu J, Li R, Cheng W, Ge S. Ozonation of acid red 18 wastewater using O3/Ca(OH)2 system in a micro bubble gas-liquid reactor. Journal of Environmental Chemical Engineering [Internet]. 2017 Feb;5(1):283–91. Available from: https://linkinghub.elsevier.com/retrieve/pii/S2213343716304432
30. Sabbar HA, Noori WO, Naje AS. Dye removal by membrane technology for wastewater treatment using a cationic carrier. Pertanika Journal of Science and Technology. 2020;28(1):353–67.
31. Cordier C, Charpin L, Stavrakakis C, Papin M, Guyomard K, Sauvade P, et al. Ultrafiltration: A solution to recycle the breeding waters in shellfish production. Aquaculture. 2019;504(October 2018):30–8.
32. Ahmed AE, Majewska-Nowak K, Ahmed M, Grzegorzek M. The separation of mineral salt from a dye-salt aqueous mixture by electrodialysis. Desalination and Water Treatment [Internet]. 2023 Dec;316(June):532–41. Available from: https://linkinghub.elsevier.com/retrieve/pii/S1944398624082225
33. Ajam NH, Jaeel AJ. Removal of reactive dyes by electro coagulation process from aqueous solution. In: AIP Conference Proceedings [Internet]. 2023. p. 030010. Available from: http://aip.scitation.org/doi/abs/10.1063/5.0140773
34. Geldasa FT, Kebede MA, Shura MW, Hone FG. Experimental and computational study of metal oxide nanoparticles for the photocatalytic degradation of organic pollutants: a review. RSC Advances [Internet]. 2023;13(27):18404–42. Available from: https://xlink.rsc.org/?DOI=D3RA01505J
35. Chen ZS. Effect of ZnO-Loading Method on Methyl Orange Removal Capacities of Expanded Graphite/ZnO Composites. Advanced Materials Research [Internet]. 2011 Jul 4;284–286:157–60. Available from: https://www.scientific.net/AMR.284-286.157
36. Amdeha E, Salem M. Facile Green Synthesis of ZnO Supported on Exfoliated Graphite for Photocatalytic Degradation of Dye under UV and Visible-Light Irradiation. Egyptian Journal of Chemistry [Internet]. 2022 May 18;65(13):0–0. Available from: https://ejchem.journals.ekb.eg/article_238068.html
37. Xiuyan Pang, Ruinian Lin* XS. Preparation of expanded graphite loaded with zinc oxide and its decolorizing performance for dye. Materials Science [Internet]. 2014 Mar 1;10(9):385–90. Available from:

https://iopscience.iop.org/article/10.1088/0031-9120/5/2/304
38. Oh W-C, Choi J-G, Zhang F-J, Go Y-G, Chen M-L. Synthesis of Expanded Graphite-Titanium Oxide Composite and its Photocatalytic Performance. Journal of the Korean Ceramic Society [Internet]. 2010 May 31;47(3):210–5. Available from: http://www.jkcs.or.kr/journal/view.php?doi=10.4191/kcers.2010.47.3.210
39. Ndlovu T, Kuvarega AT, Arotiba OA, Sampath S, Krause RW, Mamba BB. Exfoliated graphite/titanium dioxide nanocomposites for photodegradation of eosin yellow. Applied Surface Science [Internet]. 2014;300:159–64. Available from: http://dx.doi.org/10.1016/j.apsusc.2014.02.027
40. Yu X, Zhang Y, Cheng X. Preparation and photoelectrochemical performance of expanded graphite/TiO2 composite. Electrochimica Acta [Internet]. 2014;137:668–75. Available from: http://dx.doi.org/10.1016/j.electacta.2014.06.027.

مجلة كلية التربية الاساسية
كلية التربية الاساسية – الجامعة المستنصرية
Journal of the College of Basic Education Vol.31 (NO. 131) 2025, pp. 1116-1133

مراجعة موجزة عن تحضير الجرافيت الموسع ومتراكباته مع أكاسيد الفلزات في التحطم الضوئي للأصباغ

سندس هادي مرزا [1]
قسم الكيمياء، كلية التربية للعلوم الصرفة /ابن الهيثم، جامعة بغداد، العراق
[1]sundus.h.m@ihcoedu.uobaghdad.edu.iq
07707843740

مستخلص البحث:
توفر هذه المراجعة القصيرة نظرة عامة على طرق تصنيع الجرافيت الموسع (EGT) واستخدام مركباته مع أكاسيد المعادن في مجال التحلل الضوئي للأصباغ. تُمثل الأصباغ الناتجة عن تصنيع المنسوجات مشكلة تلوث بيئي كبيرة في المجاري المائية حول العالم، مما يُبرز الحاجة إلى تقنيات صديقة للبيئة وفعالة لإزالة الأصباغ من مياه الصرف الصناعي والمحلي. تُقدم تقنيات التحلل الضوئي حلاً مستدامًا ومنخفض التكلفة مع الحد الأدنى من التلوث الثانوي. تُعد المواد الكربونية، مثل الجرافيت الموسع، مفيدة في تعزيز النشاط التحفيزي. بناءً على ذلك، ستستكشف هذه المراجعة تقنيات التصنيع المختلفة للجرافيت المتمدد، وتُلخص التطورات الحديثة لمتراكبات أوكسيد الفلزات /EGT في عملية التحفيز الضوئي لتطبيقات المعالجة البيئية. خلصت هذه الدراسة إلى أن طريقة التحلل الضوئي باستخدام متراكبات الجرافيت الموسع/ أوكسيد الفلزات تُمثل خيارًا فعالًا ومنخفض التكلفة لتحلل الأصباغ.

الكلمات المفتاحية: التقشير; المسافة بين الطبقات; التحفيز الضوئي; الملوثات; حيود الأشعة السينية.
ملاحظة: هل البحث مستل من رسالة ماجستير او اطروحة دكتوراه؟ نعم: **كلا :** ✓